Article:
Li, L, Sun, H, Ding, J et al. (2017) Selective targeting of M-type potassium Kv7.4 channels demonstrates their key role in the regulation of dopaminergic neuronal excitability and depression-like behaviour. British Journal of Pharmacology, 174 (23). pp. 4277-4294. ISSN: 0007-1188

https://doi.org/10.1111/bph.14026

Selective targeting of M-type potassium channel Kv7.4 demonstrates its key role in regulating of dopaminergic neuronal excitability and depression-like behaviour

Li Li[1*], Hui Sun[1*], Jie Ding[1], Chenxu Niu[1], Min Su[1], Ludi Zhang[1], Yingmin Li[2], Chuan Wang[1], Nikita Gamper[1, 3], Xiaona Du[1], Hailin Zhang[1#]

[1]Department of Pharmacology, Hebei Medical University; The Key Laboratory of Neural and Vascular Biology, Ministry of Education, China; The Key Laboratory of New Drug Pharmacology and Toxicology, Hebei Province; Shijiazhuang, China.

[2]Department of Forensic Medicine, Hebei Medical University, Shijiazhuang, China.

[3]Faculty of Biological Sciences, University of Leeds, Leeds, UK.

Running title: Kv7.4 regulation of depression-like behaviours.

*These authors contributed equally to this work.

#Correspondence and requests for materials should be addressed to HZ (zhanghl@hebmu.edu.cn).

Abstract

Background and Purpose. The mesolimbic dopamine (DA) system originating in the ventral tegmental area (VTA) is implicated in the development of depression, and firing patterns of VTA DA neurons are key determinants in this process. Here, we describe a crucial role of the M-type potassium channel Kv7.4 in modulation of VTA DA neuronal excitability and in the development of depressive behaviour in mice.

Experimental Approach. We used Kv7.4 knock-out mice and a social defeat model of depression in combination with various electrophysiological techniques (patch clamp recording and *in vivo* single unit recordings), immunohistochemistry, single-cell PCR and behavioural analyses (social interaction time and glucose preference tests) to investigate VTA circuits involved in development of depression-like behaviour.

Key results. We demonstrate that among the Kv7 channel subunits, Kv7.4 is selectively expressed in dopamine neurons of the VTA. Using a newly identified selective Kv7.4 activator fasudil and Kv7.4 knock-out mice, we demonstrate that Kv7.4 is a dominant modulator of VTA DA neuronal excitability *in vitro* and *in vivo*. The results also demonstrate that down-regulation of Kv7.4 could be a causal factor of the altered excitability of VTA DA neurons and depression-like behaviour. Finally, the selective Kv7.4 activator fasudil strongly alleviated depression-like behaviour in the social defeat mouse model of depression.

Conclusion and Implications. Because expression of Kv7.4 in the CNS is limited, selectively targeting this M channel subunit is likely to produce less on-target side effects than non-selective M channel modulators, and thus, Kv7.4 may offer an alternative target for treating depression.

Keywords

Ventral tegmental area (VTA), dopamine (DA) neuron, social defeat model of depression, Kv7/M channel, neuron excitability

Abbreviations

DA	Dopamine
ISI	Inter-spike interval
RTG	Retigabine
SK channels	Small conductance $Ca2^{+}$-activated K^{+} channels
SN	Substantia nigra
SUS mice	Susceptible mice
TH	Tyrosine hydrolase
UNSUS mice	Unsusceptible mice
VTA	Ventral tegmental area

Introduction

Current treatments available for major depression are unsatisfactory due to their multiple side effects and low efficacy, leaving more than one-third of depressed individuals resistant to drug treatments (Wong and Licinio, 2001). In addition, antidepressants usually take several weeks to months to produce a therapeutic response. Thus, new strategies are needed to understand the pathophysiology of major depression and to develop new therapeutic treatments. Growing evidence has implicated the mesolimbic dopamine (DA) system originating in the ventral tegmental area (VTA) in the pathogenesis and treatment of depression (Dunlop and Nemeroff, 2007; Gershon *et al.*, 2007; Krishnan *et al.*, 2007). VTA DA neurons fire either tonically or in 'phasic' bursts, and these firing patterns were shown to encode different types of behaviour (Schultz, 2007). The phasic burst firing of VTA DA neurons is sufficient to drive behavioural conditioning and elicit dopamine transients with magnitudes not achieved by longer, lower-frequency spiking (Tsai *et al.*, 2009). More importantly, it has been recently demonstrated that the phasic burst firing pattern of VTA DA neurons directly controls depression-like behaviour in rodent models of depression (Chaudhury *et al.*, 2013; Tye *et al.,* 2013).

A key to understanding the molecular and cellular mechanisms underlying depression lies in deciphering the firing patterns of VTA DA neurons and identification of the main molecular players controlling such patterns (Grace *et al.*, 2007). Ionotropic NMDA receptors and

Ca^{2+}-activated K^+ (SK) channels (Creed *et al.*, 2016), HCN (Cao *et al.,* 2010; Neuhoff *et al.*, 2002) and Kir3/GIRK channels (Munoz and Slesinger*,* 2004; Padgett *et al.*, 2012) have all been suggested to play important roles in controlling either the intrinsic DA neuronal activity or the abusive drug-induced modulation of such activity. However, despite significant progress, a complete understanding of the firing patterns within the VTA circuitry and what controls these patterns is currently lacking. One emerging concept for treating depression is focused on modulation of VTA DA neuron K^+ channels (Borsotto *et al.,* 2015; Overstreet and Wegener, 2013). This concept is based on several experimental findings suggesting that K^+ channels controlling VTA DA neuron excitability may be targeted to reduce the neuronal firing and the susceptibility of mice to social depression stress (Friedman *et al.,* 2014; Krishnan *et al.*, 2007; Friedman *et al.*, 2016). Several other studies implicated K^+ channels in depression (even though some of these observations are not directly compatible), thus, genetic deletion of TREK1 K^+ channels produces an intrinsic antidepressant-like phenotype, which is not affected by further SSRI antidepressants treatments (Heurteaux *et al.*, 2006), while selective blockade of TREK1 with spadin or its analogues exerts a fast anti-depressant effect (Mazella *et al.,* 2010; Veyssiere *et al.,* 2015).

One family of K^+ channels, which is increasingly recognized for their role in controlling neuronal firing, is Kv7/KCNQ family. Kv7/KCNQ channels (Kv7.1-5) are voltage-dependent potassium channels with five members, four of which (Kv7.2–5) are abundantly expressed in the CNS (Wang *et al.*, 1998; Jentsch, 2000; Gamper and Shapiro, 2015). Kv7 channels opening leads to neuronal hyperpolarization, membrane potential stabilization and decreased excitability. This makes Kv7 channels particularly interesting as targets in neurological disorders linked to hyperexcitability, including epilepsy, anxiety, pain, migraine and addiction to psychostimulants (Brown and Passmore, 2009). Interestingly, Kv7 channels are expressed in DA neurons (Hansen *et al.*, 2006; Koyama and Appel, 2006) and have been suggested to modulate DA neuronal excitability (Drion *et al.,* 2010; Hansen *et al.*, 2008) and dopaminergic transmission (Hansen *et al.*, 2008). On the transcriptional level, Kv7.4 was found to be a predominant KCNQ gene expressed in VTA DA (Hansen *et al.*, 2006), although the functional expression and potential role of Kv7 channels in depression have not been elucidated. In this study, we provide strong evidence that Kv7.4 is a dominant Kv7 subunit in

the VTA and a potent modulator of VTA DA neuronal excitability. Due to the much more restricted expression of Kv7.4 in the CNS compared to other Kv7 subunits, targeting this channel may offer a new way to treat depression, and such a strategy could be less prone to on-target side effects than current treatments.

Materials and Methods

Animals

Kv7.4 knock-out mice ($Kv7.4^{-/-}$) were kindly provided by Prof Thomas Jentsch (FMP, MDC, Berlin, Germany) (Tatjana Kharkovets, 2006). A total of 321 male wild-type and 210 male $Kv7.4^{-/-}$ C57BL/6J mice (7-8 weeks old,Vital River, China) were used for the studies. All animals were housed at controlled temperature, humidity and lighting (12 h: 12 h light-dark cycle) and provided free access to food (provided by Experimental Animal Center of Hebei Province) and tapwater ad libitum. Animals were allowed to adapt to their housing environment for at least 7 days prior to experimentation and to the experimental room for 1 day before experiments. Animal studies were conducted in compliance with the ARRIVE guidelines (Kilkenny *et al.*, 2011; Mcgrath and Lilley, 2015). All experiments were conducted in accordance with the guides of the Animal Care and Use Committee at Hebei Medical University. The use of human tissue was approved by the Ethnic Committee of Hebei Medical University.

Cell culture

Chinese hamster ovary (CHO) K1 cells stably expressing Kv7.4 or Kv7.2/7.3 channels were maintained in F12 media (Life Technologies, USA) supplemented with 10% foetal calf serum, non-essential amino acid supplement (Gibco, USA), 600 $\mu g \cdot ml^{-1}$ G418 and 600 $\mu g \cdot ml^{-1}$ hygromycin B and incubated at 37°C in 5% CO_2. CHO K1 cells transiently transfected with Kv7.2 were grown in F12 supplemented with 10% foetal calf serum and 1% penicillin-streptomycin. Cells were grown on glass coverslips and transfected using Lipofectamine (Life Technologies, USA). Recordings were performed 24-48 h after transfection. Human Kv7.2, rat Kv7.3, and human Kv7.4 (GenBank accession numbers: AF110020, AF091247, AF105202, respectively) were kindly provided by Diomedes E. Logothetis (Virginia Commonwealth University, Richmond, Virginia, USA) and were

subcloned into pcDNA3.

VTA brain slice preparation

Brain slices containing VTA/SN were prepared as reported (Krishnan *et al.*, 2007). Mice were euthanized by pentobarbital sodium (200 mg·kg^{-1}, i.p) and brains were cut in a coronal plane, and sectioned into 250-μm-thick slices containing VTA/SN using a vibratome (VT1200S; Leica, Germany). The VTA was located stereotaxically, as described (Franklin and Paxinos, 2001), as the region dorsal to the medial mammillary nucleus or the interpeduncular nucleus, medial to the substantia nigra and ventral to the red nucleus (Shabat-Simon *et al.*, 2008). The coronal slices (250 μm) were prepared in ice-cold oxygenated (95% O_2/5% CO_2) cutting solution (in mM: KCl 2.5, NaH_2PO_4 1.25, $NaHCO_3$ 25, $CaCl_2$ 0.5, $MgCl_2$ 7, D-glucose 10 and sucrose 220; osmolarity, 295-305 mOsm) and incubated for 30 min at 36°C in oxygenated artificial cerebrospinal fluid (aCSF) (in mM: NaCl 124, KCl 3, NaH_2PO_4 1.24, $MgCl_2$ 2, $CaCl_2$ 2, D-glucose 10 and $NaHCO_3$ 26; osmolarity, 280-300 mOsm). Four coronal slices (250 μm) containing the VTA/SN were obtained from each mouse. The slices were allowed to recovery at room temperature (23-25°C) in oxygenated aCSF for at least 1 h prior to recording. Recording were made at room temperature in a recording chamber continuously perfused with oxygenated aCSF (2 ml·min^{-1}).

The human brainstem from a 45-year-old male who died of sudden cardiac death without neuropsychiatric, neurological, or neurodegenerative disease was obtained from the Department of Forensic pathology of Hebei Medical University. The use of a human tissue sample was approved by the Ethnic Committee For Human Tissue Samples.

VTA DA neuron identification

DA neurons were distinguished from non-DA neurons either by the presence of tyrosine hydroxylase (TH; single-cell PCR) or based on the functional characteristics of DA neurons as follows: i) A sag hyperpolarization potential during injection of a hyperpolarizing current pulse (sFig. 1A, 1B); ii) a typical triphasic action potential with a negative deflection, an action potential width from the start to the minimum of > 1.1 ms, and an action potential duration (from start to recovery at resting membrane rest) > 2.5 ms (sFig. 1C, 1D); iii) firing

rate less than 5 Hz (in loose patch or single unit recordings where spontaneous firing was recorded; see below); and iv) inhibition of the firing activity by dopamine (Cao *et al.,* 2010; Ungless *et al.*, 2004).

Electrophysiology

Kv7 current recordings in CHO cells expressing Kv7 were performed using the perforated patch configuration of the patch-clamp technique (amphotericin B, 250 $\mu g \cdot ml^{-1}$, Sigma, USA) at room temperature using a HEKA EPC10 patch-clamp amplifier and Patch Master software (HEKA Electronics, Germany). Currents were acquired at 10 kHz and filtered at 2.5 kHz. Patch electrodes were pulled with a micropipette puller (Sutter Instruments, USA) and polished to 2-4 MΩ resistance. The intracellular solution contained (in mM): KCl 150, $MgCl_2$ 5, HEPES 10, pH adjusted to 7.4 with KOH. Series resistance (generally below 10 MΩ) was compensated by 60-80%. The extracellular solution contained (in mM): NaCl 160, KCl 2.5, $MgCl_2$ 1, $CaCl_2$ 2, glucose 10, HEPES 20; pH adjusted to 7.4 with NaOH. Cells were held at a holding potential of -60 mV, and 1-s test pulses to -10 mV were applied every 6 s.

For whole-cell current-clamp and voltage-clamp recordings in the VTA slices, an Axopatch 1D amplifier coupled with a Digidata 1440A AD converter (Molecular Devices, USA) was used, and the data were analysed using Clampex 10.3 (Molecular Device, USA) and OriginPro 8.5 software (Origin Lab Corporation, USA). For Kv7/M current recordings, neurons were held at -10 mV and 1-s square pulses to -50 mV were delivered repeatedly at 20-s intervals. The M current was measured as the instantaneous deactivating tail current at the beginning of a voltage step to -50 mV. Whole-cell patch-clamp recordings were made with glass electrodes (4-6 MΩ) using an internal solution containing (in mM): K-methylsulfate 115, KCl 20, $MgCl_2$ 1, HEPES 10, EGTA 0.1, MgATP 2 and Na_2GTP 0.3, pH adjusted to 7.4 with KOH. The extracellular solution was the aCSF. A cell-attached "loose-patch" (100-300 MΩ) (Burlet *et al.*, 2002) recordings were also used to record spontaneous firing of DA neurons. In this case, the pipette solution contained aCSF.

Single unit recordings were used to record the spontaneous firing of VTA DA neurons *in vivo* based on a previously reported method (Mameli-Engvall *et al.*, 2006). Briefly, mice were anaesthetized by 4% chloral hydrate (400 $mg \cdot kg^{-1}$, i.p.); the coordinates for the VTA were

2.92-3.16 mm from the anterior fontanel, 0.50-0.70 mm lateral from the midline and 4.20-5.00 mm ventral from the cortical surface. DA neurons were identified by their characteristics of the action potentials (typical triphasic action potentials with a negative deflection: the action potential width from the start to the minimum trough of ≥ 1.1 ms, a characteristic long duration (> 2 ms) and a slow firing rate (< 10 Hz) (Cao *et al.,* 2010) (Fig. 3F). The presence of burst firing (as opposed to tonic firing) was identified by the following criteria: 1) the start of a burst was registered when two consecutive spikes fired within 80 ms; 2) the end of the burst was registered when the interspike interval (ISI) exceeded 160 ms (Cao *et al.,* 2010); and 3) a neuron was considered as burst-firing if it fired at least one burst within 3 min. Electrical signals were amplified and filtered (10-4K Hz) by the Axoclamp 900A preamplifier and recorder by the Digidata 1440A AD converter (Molecular Devices, USA); the data were analysed by Clampfit 10.3 (Molecular Devices, USA).

The effect of 0.9% saline (vehicle), fasudil (20 $mg \cdot kg^{-1}$) or retigabine (RTG) (10 $mg \cdot kg^{-1}$) on the firing activity of VTA DA neurons recorded using single unit recordings was assessed 10 min after intraperitoneal injection (i.p.) or 5 min after direct VTA local pressure (5 - 15 psi) injection (see Fig. 6 legend for detail). The effects of drugs on the following parameters were analysed: (i) average firing rates (Hz); ii) corresponding ISI (ISI histograms were plotted for at least 5 min of continuous recording); iii) percentage of cells displaying burst firing (number of burst firing cells/ number of all cells recorded × 100%); iv) average number of spikes in a burst (number of spikes in burst/ number of burst events); and v) percentage of spikes in bursts (number of spikes in bursts/total number of spikes × 100%).

Chronic social defeat stress

The mouse social defeat model of depression was established based on the protocols reported previously (Krishnan *et al.*, 2007). Briefly, the C57BL/6 mice were subjected to attack by a CD1 mouse for 10 min a day for 10 days. CD1 retired breeders were selected before the test, and the fiercest CD1 mice were excluded in the following experiment. In addition, the intensity of attack stimuli was minimized to produce stable depressive behaviour. To minimize harm and avoid physical injury, plastic dividers were set when C57BL/6J mice displayed submissive behaviour, including immobility, crouching, trembling, fleeing and upright posture. On day 1 and day 11, the weight was recorded, and a sucrose preference test

was performed as follows. Mice were individually accommodated in cages with two drinking water bottles for 24 h (food provided *ad libitum*). The animals were then deprived of water and food for 12 h. After this period, two drinking bottles were re-introduced with one containing 0.8% sucrose solution and the other filled with drinking water. Twelve hours later, the bottles were removed and weighted. Sucrose preference was calculated as a percentage [(weight of sucrose solution consumed / total weight of liquid consumed from two bottles) × 100%]. On day 13, the social interaction test was carried out. The C57BL/6 mice were placed in an interaction test box and allowed to move freely for 2.5 min in the absence or presence of an unfamiliar caged CD1 mouse. The time the test C57BL/6 mice spent in the interaction zone and in the corner zone (see sFig. 2A, 2B) was analysedanalyse (sFig. 2C). Subgroups of susceptible and unsusceptible mice were identified. The animals were qualified as susceptible to depression-like behaviour (SUS) if they spent significantly less time in the interaction zone while a CD1 mouse was present than while a CD1 mouse was not present. Animals that did not respond to the presence of a CD1 mouse by reduced interaction time were qualified as unsusceptible mice (UNSUS). Sucrose preference was an additional test used to determine depression susceptibility (see below). Animals were divided into groups randomly. Experimenters were blinded to the drug treatment while performing the tests.

Cannula implantation for direct injection of drugs into the VTA

Mice were anaesthetized by intraperitoneal injection of 8% chloral hydrate (400 $mg \cdot kg^{-1}$, i.p) and placed into a stereotaxic apparatus. Mice were bilaterally implanted with a stainless 26-gauge cannula fitted with obturators (Plastics One) targeting directly above the VTA with the following coordinates: anteroposterior, 3.08 mm; lateral, 0.50 mm; dorsoventral, 4.20 mm. The cannulae were secured with dental cement; and the mice were then singly housed and allowed to recover for 3 days. After the surgery, the mice were housed at 28℃ for 8 h to maintain their body temperature. All instruments were autoclaved, and the skin of the animals was sterilized with alcohol and iodine to prevent infection after surgery. The animals were placed in a cage with clean sawdust bedding and provided free access to fresh water and food (provided by Experimental Animal Center of Hebei Province).

Western blotting

Mice were euthanized by pentobarbital sodium (200 mg·kg^{-1}, i.p) and perfused transcardially with 0.01 m ice-cold PBS. Brains were rapidly removed and VTA punches (2 mm diameter, 2 mm thick) from these mice were sonicated in 1% SDS lysis buffer containing protease inhibitor and centrifuged at 4°C for 30 min at 17220 g. Protein samples (40 mg) were separated by 10% SDS-PAGE for 1.5 h and transferred to a nitrocellulose membrane for 2 h in 20% transfer buffer. Membranes were then blocked for 1 hour at room temperature in TBST (TBS and 0.1% Tween-20) with 5% nonfat milk (Sigma, USA) and then were incubated overnight at 4°C with primary antibody against Kv7.4 (1:1000, Alomone Labs, USA) or β-tubulin (1:10000, Abcam, UK) diluted in TBST. Membranes were washed with TBST for 3 × 10 min, incubated with goat anti-rabbit (1:5000, Rockland, USA) or goat anti-mouse (1:7500, Rockland, USA) secondary antibodies for 1 h at room temperature, and washed with TBST for 2 × 10 min followed by another 10-min wash with TBS. Membranes were imaged using an Odyssey infrared imaging system (LI-COR, USA); the integrated optical density of each band was measured using ImageJ software (National Institutes of Health, USA).

Immunofluorescence

For experiments shown in Fig. 1D, mice were euthanized by pentobarbital sodium (200 mg·kg^{-1}, i.p) and perfused transcardially with 0.01 m ice-cold PBS, followed by ice-cold PBS containing 4% paraformaldehyde (PFA). The brain was removed, fixed in 4% PFA at 4°C for 48 h and embedded in paraffin. Paraffin coronal VTA/SN slices (5 μm) were mounted on glass slides. Coronal VTA/SN slices located at 1.40 to 0.50 mm from lambda. Slices were dewaxed in xylene and rehydrated in alcohol. Antigen retrieval was achieved by microwave heating (three times for three min) of the brain slices. Sections were blocked with 10% goat serum (Biological Industries, Israel) in PBS and incubated overnight with a mixture of mouse anti-TH (1:100, Merck Millipore, Germany, Cat# MAB318 Lot#, RRID: AB_2201528) and rabbit anti-Kv7.4 (1:100, AlomoneLabs, Israel, Cat# APC-164 Lot#, RRID: AB_2341042) antibodies. Sections were then washed with PBS six times (5 min) and incubated in FITC-conjugated AffiniPure goat anti-mouse IgG (Jackson ImmunoResearch, USA, Labs

Cat# 115-095-003, RRID:AB_2338589; 1:200) and Cy3-conjugated AffiniPure goat anti-rabbit IgG (Jackson ImmunoResearch, USA; 1:200, Labs Cat# 111-165-003, RRID:AB_2338000) for 30 min at 37°C. Sections were then washed six times (5 min) with PBS. Subsequently, sections were counterstained with 4,6-diamidino-2-phenylindole (DAPI, Sigma, USA) to identify nuclei for 20 min at room temperature, and washed three times with PBS (5 min). Finally, slices were mounted with Prolong Gold antifade reagent (Life Technologies, USA).

For experiments shown in Fig. 1A, the brain was fixed in 4% PFA at 4°C for 24 h and embedded in 30% sucrose for 24 h. Coronal VTA/SN slices (60 µm) were cut using a vibratome (VT1200S; Leica, Germany). Sections were blocked with 10% goat serum overnight with a mixture of two primary antibodies: mouse anti-TH (1:100, Merck Millipore, Germany) and rabbit anti-Kv7.2 (1:100, Santa Cruz, CA, Cat# sc-7793, RRID: AB_2296585), goat anti-Kv7.3 (1:100, Santa Cruz, CA, Cat# sc-7794 Lot#, RRID: AB_2131714), rabbit anti-Kv7.4 (1:100, AlomoneLabs, Israel), or rabbit anti-Kv7.5 (1:50, Santa Cruz, CA, Cat# sc-50416 Lot#, RRID:AB_2131834). Sections were then washed with PBS six times (5 min) and incubated in a mixture of two secondary antibodies: FITC-conjugated AffiniPure goat anti-mouse IgG (Jackson ImmunoResearch, USA; 1:200) and Cy3-conjugated AffiniPure goat anti-rabbit IgG (Jackson ImmunoResearch, USA; 1:200) for 30 min at 37°C. Sections incubated with anti-Kv7.3 antibody were incubated in Cy5-conjugated AffiniPure donkey anti-goat IgG (Jackson ImmunoResearch, USA, Labs Cat# 705-175-147, RRID:AB_2340415; 1:400) and FITC-conjugated AffiniPure donkey anti-mouse IgG (Jackson ImmunoResearch, USA, Labs Cat# 715-095-151, RRID:AB_2335588; 1:400).

Images were taken using a Leica TCS SP5 confocal microscope (Leica, Germany) equipped with laser lines for DAPI (800 nm, Ti-sapphire coherent pulsed), FITC (Argon 488), cy3 (HeNe 543) and cy5 (red diode 637 nm). Images were analysed with LAS-AF-Lite software (Leica).

Tissue blocks of the brainstem from human brain were fixed in 4% PFA at 4°C and embedded in paraffin. Slices were dewaxed and rehydrated. Antigen retrieval and incubation with antibodies were performed by the same protocol used for mouse samples.

Single-cell PCR

Neurons were aspirated into a patch pipette at the end of electrophysiological recordings. The electrode tip was then broken into a PCR tube containing 1 µl of oligo-dT (50 mM) and 1 µl of dNTP mixture (10 mM). The mixture was heated to 65°C for 5 min to denature the nucleic acids and then placed on ice for 1 min. Single-strand cDNA was synthesized from the cellular mRNA by mixing 2 µl of 5× PrimeScript II buffer (50 mM), 0.5 µl of RNase inhibitor (40 $U \cdot \mu l^{-1}$) and 1 µl of PrimeScript II RTase (200 $U \cdot \mu l^{-1}$) and then incubating the mixture at 50°C for 50 min. Synthesis of single-cell cDNA was performed using a C1000 Touch thermal cycler-CFX96 Real-time PCR system (California, USA). First strand synthesis was executed at 95°C (5 min) followed by 35 cycles (95°C for 1 min, 56°C for 45 s, 72°C for 50 s) and a final 10 min elongation at 72°C by adding the specific "outer" primer pairs to each PCR tube (final volume 25 µl). Then, 2 µl of the product of the first PCR was used in the second amplification round by using the specific "inner" primer (final volume 50 µl). The second amplification round consisted of heating the samples to 95°C for 5 min followed by 30 cycles (95°C for 1 min, 54-62°C for 45 s, 72°C for 50 s) and 10 min elongation at 72°C. The products of the second round of PCR were analysed in 2.5% agarose gels and stained with ethidium bromide. A PrimeScriptTM II 1 st Strand cDNA Synthesis Kit and GoTaq Green Master Mix were obtained from Takara-Clontech (Kyoto, Japan) and Promega (Madison, USA), respectively.

The "outer" primers (from 5′ to 3′) as follows:

GAPDH	AAATGGTGAAGGTCGGTGTGA ACG (sense)	AGTGATGGCATGGACTGTGGT CAT (antisense)
TH	ATACAAGCAGGGTGAGCCAA	TACACCGGCTGGTAGGTTTG
Kv7.2	TCTCCTGCCTTGTGCTTTCT	GCATCTGCGTAGGTGTCAAA
Kv7.4	CCCGGGTGGACCAAATTGT	AGCCCTTCAGTCCATGTTGG

The “inner” primers (from 5′ to 3′) as follows:

GAPDH	GCAAATTCAACGGCACAGTC AAGG	TCTCGTGGTTCACACCCATCA CAA
TH	TTCTTGAAGGAACGGACTGGC	TCAGCCAACATGGGTACGTG
Kv7.2	AGGAAGCCGTTCTGTGTGAT	GCAGAGGAAGCCAATGTACC
Kv7.4	ATGGGGCGCGTAGTCAAGGT	GGGCTGTGGTAGTCCGAGGTG

qRT-PCR

Total RNA from the VTA of mice was extracted using a mirVana miRNA Isolation Kit (Invitrogen, USA) according to the manufacturer’s recommendations. The RNA was reverse transcribed into cDNA using a PrimeScript™ RT reagent kit with gDNA Eraser (TAKARA, RR047A, Japan). qRT-PCR of Kv7.4 and glyceraldehyde-3-phosphate dehydrogenase (GAPDH) was performed using an ABI PRISM 7300 Sequence Detection System (Applied Biosystems, USA) with a SYBR® Premix Ex Taq™ II (TliRNaseH Plus) kit (TAKARA, RR820A, Japan). The relative amounts of transcripts were normalized to GAPDH; the relative RNA expression levels were calculated using the following equation: relative gene expression = $2^{-(\Delta Ct\ sample\ -\ \Delta Ct\ control)}$. The following primers were used.

Kv7.4 5’- ATGGGGCGCGTAGTCAAGG T-3’ (sense);
5’- GGGCTGTGGTAGTCCGAGGTG -3’ (antisense);

GAPDH 5’- GGTGAAGGTCGGTGTGAACG -3’ (sense);
5’- CTCGCTCCTGGAAGATGGTG -3’ (antisense).

Drugs

Retigabine and Y-27632 were from Sigma-Aldrich (China). Fasudil was from the National Institute for the Control of Pharmaceutical and Biological Products (Beijing, China). XE991 dihydrochloride was from Alomone Labs (Jerusalem, Israel). RL-648_81 was synthesized by the Department of New Drugs Development, School of Pharmacy, Hebei Medical University. All solutions were prepared freshly on the test day.

Statistics

Sample size was determined through power analysis using preliminary data obtained in our laboratory with the following assumptions: 'α' of 0.05 (two-tailed) and power of 90%. Data are reported as the means ± s.e.m. Statistical analysis of differences between groups was carried out by Student's paired or unpaired t-tests, as appropriate. For data that failed a normality test, a paired sample Wilcoxon signed rank test or Mann-Whitney tests was used. Multiple groups were compared using one-way ANOVA with Bonferronni's correction or by Kruskal-Wallis ANOVA with a Mann-Whitney test. P values ≤ 0.05 were accepted as significant. Fisher's exact test was used to compare population size. Data analysis was carried out using OriginPro 9.1 (OriginLab Corp., Northampton, MA). The data and statistical analysis comply with the recommendations on experimental design and analysis in pharmacology (Curtis, *et al.*; 2015).

Nomenclature of Targets and Ligands

Key protein targets and ligands in this article are hyperlinked to corresponding entries in http://www.guidetopharmacology.org, the common portal for data from the IUPHAR/BPS Guide to PHARMACOLOGY (Southan et al., 2016), and are permanently archived in the Concise Guide to PHARMACOLOGY 2015/16 (Alexander et al., 2015).

Results

Kv7.4 channels are selectively expressed in VTA DA neurons

It has been shown that among the Kv7/KCNQ isoforms, Kv7.4 is the predominant KCNQ gene transcript present in the midbrain VTA (Hansen *et al.*, 2006). We first performed detailed analysis of protein and mRNA expression of Kv7/KCNQ isoforms in the midbrain of mice, with a special interest in the expression of these Kv7 channels in DA neurons (identified by the expression of tyrosine hydrolase, TH). In the immunofluorescence study (Fig. 1A, C), Kv7.2-Kv7.5 were found to be differentially expressed in the DA neurons of the VTA and the substantia nigra (SN) of the mouse midbrain. Overall, among the four Kv7 isoforms, Kv7.4 was more selectively expressed in VTA than SN DA neurons. Thus, while 66% of TH-positive (DA) neurons in the VTA expressed Kv7.4, only 27% of these neurons in the SN expressed this channel ($P < 0.001$; Fisher's exact test). Among the other Kv7 subunits,

only Kv7.5 exhibited a slightly higher incidence of expression in the VTA compared to the SN (33% *vs.* 22% neurons, respectively, $P > 0.05$; Fig. 1C), yet the proportion of Kv7.5-positive neurons in the VTA was still significantly lower compared to the proportion of Kv7.4-positive neurons (33% *vs*. 66% of neurons respectively, $P < 0.001$; Fig. 1C). Interestingly, Kv7.2 significantly more frequently expressed in SN neurons (62%) compared to VTA neurons (62% *vs* 45%; $P < 0.05$; Fig. 1C). Kv7.3 and Kv7.5 were expressed in much smaller proportions of VTA DA neurons (Fig. 1C).

Similarly, in a single-cell PCR study (Fig. 1B, C), Kv7.4 was also found to be more selectively expressed in VTA DA neurons (63% *vs* 19% in SN; $P < 0.001$), whereas the expression of Kv7.2 was more abundant in SN DA neurons (55% *vs* 34% in VTA, $P = 0.12$; Fig. 1C). Kv7.4 was absent in VTA DA neurons of the Kv7.4 knockout mice ($Kv7.4^{-/-}$; Fig. 1D). Kv7.4 expression was also found in human VTA DA neurons (Fig. 1E). Taken together, the results presented in Fig. 1 demonstrate that, while several Kv7 isoforms are expressed in VTA DA neurons, Kv7.4 is the predominant subunit.

Fasudil selectively activates Kv7.4 currents in VTA DA neurons

We next aimed to selectively modulate Kv7.4 channels to regulate the excitability of VTA DA neurons. Our first goal was to identify a Kv7.4-selective modulator. In a separate investigation of the effects of a Rho-associated protein kinase (Uehata *et al.*, 1997) inhibitor fasudil (1-[5-isoquinolinesulfonyl]-homopiperazine, HA-1077, AT-877) in the cardiovascular system, we discovered that fasudil is also a selective opener of Kv7.4 channels (Zhang *et al.*, 2016). In CHO cells that exogenously express Kv7.4, fasudil enhanced Kv7.4 currents in a concentration-dependent manner but did not affect Kv7.2 currents (Fig. 2A1-A3). RTG, a prototypic non-selective opener of Kv7 channels (Tatulian *et al.*, 2001) enhanced both Kv7.4 and Kv7.2 currents, which were inhibited by the Kv7 blocker XE991 (Fig. 2A1-A2). Importantly, fasudil did not activate heterologously expressed Kv7.2/Kv7.3 multimeric channels (sFig. 3), which are the major correlates of the M-type current in the CNS (Wang *et al.*, 1998). Fasudil did not affect Kv7.1 and Kv7.3 channels but did activate Kv7.4/Kv7.5 multimers (Zhang *et al.*, 2016). Thus, we concluded that fasudil is a selective activator of Kv7.4-containing homo- and hereromeric Kv7 channels.

We then tested the effect of fasudil on K^+ currents in VTA neurons. We recorded Kv7/M-like currents from VTA/SN slices of adult mice (6-8 weeks). The currents were recorded using the protocol shown in the right panel of Fig. 2B1 as the characteristic slow deactivating tail current at -50 mV, which is defined as the 'M current' and is mostly conducted by Kv7 channels (Koyama and Appel, 2006). Accordingly, 45.6 ± 6.0% of the deactivating current was inhibited by XE911 (3 μM; Fig. 2B1). In these experiments, we used well-characterized hallmarks to select DA neurons (sFig. 1; see Methods for details). As it has been reported and consistent with our results shown in Fig. 1, the majority (~70%) of VTA neurons are DA neurons, with a small population of GABAergic neurons and glutamatergic neurons (Nair-Roberts *et al.*, 2008). Due to these considerations, the selection criteria, and the subsequent confirmation by post-recording single-cell RT-PCR (see below), most of the recorded neurons were indeed DA neurons.

Fasudil induced a prominent increase in M-like currents in VTA DA neurons (Fig. 2B1, 2C), with potency similar to that recorded in CHO cells overexpressing exogenous Kv7.4 (Fig. 2B3). Deletion of Kv7.4 ($Kv7.4^{-/-}$ mice) greatly reduced the basal Kv7/M-like K^+ currents and completely abolished the fasudil-induced Kv7/M-like K^+ currents in VTA DA neurons (Fig. 2B2, B3, 2C). These results strongly suggest that i) fasudil selectively activates Kv7.4 and ii) Kv7.4 is the functionally dominant Kv7 channel subunit in VTA DA neurons. The residual small basal currents and the RTG-activated currents in the $Kv7.4^{-/-}$ mice (Fig. 2C) could arise from other Kv7 subunits (Fig. 1A-C). We also tested the effects of fasudil on Kv7/M-like currents of SN DA neurons. Unlike in VTA DA neurons, fasudil did not induce significant activation of Kv7/M currents in SN neurons (from 94.1 ± 0.7 pA to 94.4 ± 0.2 pA by 100 μM fasudil treatment, n = 22, $P > 0.05$, paired t test).

Kv7.4 activity controls the excitability of VTA DA neurons

Next, we tested the influence of Kv7.4 on the excitability of VTA DA neurons. Excitability was recorded using a loose cell-attached patch method (Williams and Wozny, 2011; Burlet *et al.*, 2002) from brain slices of WT and $Kv7.4^{-/-}$ mice. We recorded from VTA neurons located primarily in the lateral part of the VTA, as projections from this portion of VTA DA neurons are more likely to be involved in depression-like behaviour (Barbara *et al.*, 2016).

The placement of recording electrodes and the positions of recorded neurons are shown in the schematic of Fig. 3A2 (top). We recorded the spontaneous firing of VTA neurons with action potential wave form characteristics of DA neurons (sFig. 1, Methods) (Fig. 3A1, right panel). Fasudil (10 μM) significantly reduced the average firing frequency of VTA neurons (Fig. 3A1, D). Post-recording single-cell PCR analysis confirmed that the inhibitory effect of fasudil resulted from activation of Kv7.4, as fasudil only inhibited firing in VTA DA neurons that expressed Kv7.4 but did not inhibit firing in Kv7.4-negative neurons (Fig. 3A2). The DA phenotype of these neurons was additionally confirmed by TH expression (Fig. 3A2).

Fasudil did not affect the firing frequency in VTA DA neurons of Kv7.4$^{-/-}$ mice (Fig. 3B, 3D). Consistent with the limited expression of Kv7.4 in the SN, the firing of DA SN neurons was not significantly affected by fasudil (Fig. 3C, 3D). On the other hand, the firing of both VTA and SN neurons was inhibited by non-selective Kv7 opener, RTG and by a selective Kv7.2 opener RL-648-81 (10 μM) (Kumar *et al.*, 2016) (Fig 3A-3D); the effect of RTG was persistent in Kv7.4$^{-/-}$ mice (Fig 3B, 3D). These data support our finding that Kv7.2 is present in both VTA and SN neurons (Fig. 1). In further evidence supporting a role of Kv7.4 in controlling DA neuron excitability, we found that the absence of Kv7.4 (Kv7.4$^{-/-}$) renders VTA DA neurons with a higher spontaneous firing frequency (Fig. 3E, 1.8 ± 0.2 Hz vs 1.1 ± 0.1 Hz, for Kv7.4$^{-/-}$ and WT mice respectively, $P < 0.05$, one-way ANOVA). Furthermore, DA neurons in the SN of WT mice, which have limited expression of Kv7.4, also had a higher firing frequency compared to VTA DA neurons from WT mice (Fig. 3E, 1.10 ± 0.1 Hz *vs.* 1.96 ± 0.27 Hz, for the VTA and SN respectively, $P < 0.05$, one-way ANOVA). On the other hand, no difference in firing frequency between SN neurons from WT mice and Kv7.4$^{-/-}$ mice was found (Fig. 3E).

We further tested the effects of Kv7 channel modulation on the excitability of VTA DA neurons using current-clamped whole-cell recordings from VTA slices. In these experiments, the following parameters were recorded: i) the resting membrane potential (RMP) (sFig. 4A), ii) the induced action potential firing frequency (sFig. 4B, C), and iii) the spontaneous firing rates (sFig. 4D). Comparison of the above parameters between WT and Kv7.4$^{-/-}$ mice clearly indicated that Kv7.4 constitutively modulates the excitability of VTA DA neurons.

Finally, the contribution of Kv7.4 in the regulation of VTA DA neuronal excitability was also

assessed in an *in vivo* setting. The spontaneous firing of VTA DA neurons was recorded *in vivo* using an extracellular single unit recording method (Fig. 3F). In this recording paradigm, two patterns of firing (Fig. 3F, expanded traces) were often recorded from the same neurons, the tonic firing (Fig. 3F1) and burst firing (Fig. 3F2; see Method for detail), and both total firing frequency and the burst firing properties were analysed (Krishnan *et al.*, 2007). In WT mice, intraperitoneally injected fasudil (i.p.; 20 $mg \cdot kg^{-1}$) reduced the total firing frequency (Fig. 3G1, G2) and the percentage of spikes in bursts (Fig. 3G3) and increased the ISI (Fig. 3G1). In stark contrast, in Kv7.4$^{-/-}$ mice, neither the total firing frequency nor the percentage of spikes in bursts was affected by fasudil treatment (Fig. 3G2, G3).

The role of Kv7.4 in the development of a depression-like phenotype in a social defeat model of depression

Increased activity of VTA DA neurons is directly related to depression-like behaviours in the social defeat model of depression (Cao *et al.,* 2010; Chaudhury *et al.*, 2013; Friedman *et al.,* 2014.; Krishnan *et al.*, 2007). Because Kv7.4 plays a significant role in controlling the excitability of VTA DA neurons, we investigated whether altered Kv7.4 channel activity is a causal factor for the increased excitability of VTA DA neurons observed in the social-defeat mice model. For this, we first established a model of social defeat (Fig. 4A, sFig. 2; see Methods for detail). The depression-like state of mice was verified by reduced sucrose preference (Fig. 4B) and reduced social interaction time when an 'aggressor' CD1 mouse was present (Fig. 4C). Mice that exhibited reduction in both parameters were defined as 'susceptible mice' (SUS). Mice with both parameter unaltered were identified as 'unsusceptible mice' (UNSUS) (Chaudhury *et al.*, 2013; Krishnan *et al.*, 2007).

Consistent with the previous reports, the firing activity of VTA DA neurons, recorded using the *in vivo* single unit recording method, was higher in SUS mice than in control and UNSUS mice (3.79 ± 0.17 Hz, n = 98 in SUS mice *vs.* 2.18 ± 0.25 Hz, n = 27 in control mice, or 2.34 ± 0.32 Hz, n = 10 in UNSUS mice) (Fig. 4D). Importantly, burst firing also increased in SUS mice compared to control and UNSUS mice (36.35 ± 3.02%, n = 43 in SUS mice vs. 22.35 ± 2.54%, n = 18 in control mice, or 21.35 ± 4.25%, n = 10 in UNSUS mice) (Fig. 4E); this was reported to be an important determinant of depression-like behaviour in mice

(Chaudhury *et al.*, 2013; Krishnan *et al.*, 2007).

We then recorded Kv7/M currents of VTA DA neurons from SUS and UNSUS mice. As shown in Fig. 4F, Kv7/M currents were reduced in SUS mice compared with control and UNSUS mice (Fig. 4). To test if the reduced Kv7/M currents were due to down-regulation of Kv7.4 expression, we first measured Kv7.4 mRNA levels using qPCR. The results shown in Fig. 4G demonstrated that indeed the mRNA levels of Kv7.4 were indeed lower in the VTA of SUS mice compared with control and UNSUS mice. We also performed a correlation analysis and found that the firing frequency of VTA DA neurons was strongly negatively correlated with the expression level of Kv7.4 mRNA (R^2 = 0.75), regardless of the SUS/UNSUS phenotype (Fig. 4H). We also measured the levels of Kv7.4 protein in the VTA and found that Kv7.4 protein abundance in the VTA of SUS mice was similarly reduced compared to the levels in control and (to a lesser extend) UNSUS mice (Fig. 4I), in good agreement with the RT-PCR data.

Fasudil reduces VTA DA neuronal excitability and reverses depression-like behaviour

The results thus far allowed us to hypothesize that fasudil, by activating Kv7.4 in VTA DA neurons, should be able to ameliorate the increased excitability of VTA DA neurons and the related depression-like behaviour in a social defeat mouse model of depression. We used several approaches to test this hypothesis. First, we used the cell-attached recordings of VTA DA neuronal firing of control, SUS and UNSUS mice. Indeed, fasudil reduced the firing rate of VTA DA neurons in SUS mice by 31.6 ± 12.2% (from a basal value of 2.53 ± 0.39 Hz, n = 12; Fig. 5A1, 5A2), although it was less efficacious than in control mice (42.2 ± 13.5% reduction from a basal value of 1.46 ± 0.25 Hz, n = 8; Fig. 5A1, 5A2). These results are consistent with reduced (but not abolished) Kv7.4 channel expression and reduced M current amplitudes in the VTA DA neurons of SUS mice.

In further experiments, using *in vivo* single unit recordings we found that the total firing activity of DA neurons in the VTA of WT mice was decreased and that ISI increased significantly following intraperitoneal injection of fasudil (20 $mg \cdot kg^{-1}$) or RTG (10 $mg \cdot kg^{-1}$), but not vehicle (0.9% saline, 0.15 ml; Fig. 5B and 5C). Similarly, burst firing was also decreased after treatment with fasudil and RTG (Fig. 5D, E). However, in Kv7.4$^{-/-}$ mice, fasudil failed to affect the firing of VTA DA neurons whereas RTG remained to be effective

albeit with a reduced efficacy (Fig. 5C).

Most importantly, the social defeat-induced avoidance behaviour of WT SUS mice was reversed by acute administration (i.p.) of fasudil and RTG. Specifically, in vehicle-treated SUS mice, introduction of the unfamiliar CD1 mouse into the interaction test box (sFig. 2B; Methods) induced an avoidance response from the tested mice. Thus, the time that the tested mice spent in the interaction zone was reduced (Fig 5F), indicating depression-like behaviour induced by social defeat. However, when WT SUS mice were injected with either RTG or fasudil, the time that the tested mice spent in the interaction zone in the presence of the 'aggressor' CD1 mouse was not significantly different from the control period (without the 'aggressor'). This indicates that Kv7 channel openers indeed abolished the avoidance reaction to the introduction of the unfamiliar CD1 mice, indicating a reversal of depression-like social interaction deficit. It should be noted that when a CD1 mouse was absent, the time spent in the interaction zone for SUS mice from vehicle, fasudil or RTG treatment groups (Fig. 5F) was not significantly different (59.15 ± 5.60 s, n = 13 in vehicle group; 48.54 ± 4.00 s, n = 13 in fasudil group; 48.43 ± 5.75 s, n = 7 in RTG group; $P = 0.41$ vehicle *vs.* fasudil, $P = 0.61$ vehicle *vs.* RTG and $P = 0.99$ fasudil *vs.* RTG; One-way ANOVA). In Kv7.4$^{-/-}$ mice however, fasudil failed to affect the behavioural response of SUS mice to the presence of the CD1 'aggressor' (Fig. 5G); RTG, however, was still effective (Fig. 5G) but the effect was highly variable. Notably, under RTG treatment, WT, as well as Kv7.4$^{-/-}$ mice became less active e.g., their mobility in the open field test was significantly reduced (sFig. 5B, C); this was consistent with the previously reported sedative effect of RTG (Hayashi *et al.*, 2014). Fasudil on the other hand, did not affect the general activity of the mice of either genotype (sFig. 5B, C). These data suggest that RTG, but not fasudil, exerts a central, Kv7.4-independent sedative effect.

To provide direct evidence that fasudil, when administered systemically through intraperitoneal injection, reversed the fault in social interaction of the social defeat mice through action on VTA DA neurons, fasudil was also infused directly onto the VTA through a cannula implanted to delver mounted on the top of the VTA (Fig. 6E, see Methods for details). Different concentrations of fasudil (and RTG) were first tested to select a concentration of the drug to obtain an effect on VTA DA neuronal firing activity comparable

to that recorded after systemic administration. Ultimately, 200 μM was chosen to further test the effects of localized drug delivery on social interaction behaviour. At 200 μM both fasudil and RTG induced significant inhibition on VTA neuron firing activity (Fig. 6A-C). Social interaction was tested at two time points after fasudil was administered, 5 min and 40 min; a time-matched (5 min) vehicle control was also tested (Fig. 6D). At both time points, local VTA infusion of fasudil or RTG abolished 'aggressor' avoidance and normalized the time a mouse spent in the interaction zone (Fig. 6F) and in the corner zone (Fig. 6G) in the presence of a CD1 'aggressor'. Thus, similar to systemic administration, direct local injection of fasudil into the VTA also reversed the depression-like social interaction behaviour.

Discussion

Here, we demonstrate that 1) Kv7.4 is selectively expressed in VTA DA neurons and represents a major Kv7/M channel subunit in in these cells; 2) Kv7.4 plays a key role in the regulation of VTA DA neuronal excitability; 3) down-regulation of Kv7.4 strongly contributes to the increased excitability of the VTA DA neurons and, thus, may trigger the development of a depression-like state in mice. Finally, 4) fasudil is a selective Kv7.4 opener, and its targeted modulation of Kv7.4 significantly improves depression-like behaviour in the social defeat mouse model of depression. Since VTA DA neuronal excitability is critical in the development of depressive state (Chaudhury *et al.*, 2013; Tye *et al.,* 2013), Kv7.4 represents a promising target for developing new antidepressants. In this regard, our finding of selective activation of Kv7.4 and subsequent Kv7.4-dependent reversal of a depression states by fasudil is particularly exciting. Kv7.4 has a much more restricted expression in the CNS compared to Kv7.2 and Kv7.3 (Hansen *et al.*, 2006; Hansen *et al.*, 2008). This reduces the risk of on-target side effects of a selective Kv7.4-based therapy compared to broad-spectrum M channel targeting with currently available drugs such as RTG. Consistent with this hypothesis, in our behavioural experiments, fasudil did not produce a sedative effect, while RTG was clearly sedative (sFig. 5). The fact that fasudil is already a clinically approved drug used for the treatment of cerebral vascular spasm (Uehata *et al.*, 1997), makes these findings even more relevant. Importantly, the anti-excitatory effects of fasudil in the VTA are likely to be independent of its Rho kinase inhibitior activity, since an another

unrelated Rho kinase inhibitor, Y-27632, did not affect the excitability of VTA DA neurons recorded either both *in vitro* and *in vivo* (sFig. 6).

The argument that K^+ channel openers can be used to treat depression is based on the rationale that increased VTA DA neuronal excitability is linked to the development of depression, and thus, K^+ channel openers may help to reverse the over-excitable state of the VTA. The VTA activation theory is applicable to the social defeat depression model (Cao *et al.,* 2010; Chaudhury *et al.*, 2013; Friedman *et al.,* 2014; Krishnan *et al.*, 2007). In this model of depression, it is believed that increased phasic firing of VTA DA neurons *via* increased release of BDNF in the nucleus accumbens (NAc) confers individual susceptibility to stressful stimulation (Chaudhury *et al.*, 2013; Krishnan *et al.*, 2007). Elevated K^+ channel activity could counteract the increased VTA DA activity and alleviate depressive behaviour (Friedman *et al.,* 2014; Krishnan *et al.*, 2007; Friedman *et al.*, 2016). Thus, the VTA DA activation theory implicates the increased burst firing rates of VTA-NAc DA neurons as a crucial mediator of social-stress-induced depressive behaviour (Walsh and Han, 2011). Our results conform well to this theory: the targeted activation of Kv7.4 K^+ channels reduced the increased excitability of VTA DA neurons and at the same time improved the depression-like behaviour of socially defeated mice. Importantly, the Kv7.4-selective opener produced much fewer side-effects compared to the broad-spectrum Kv7 channel opener RTG.

The elevated neuronal excitability in VTA DA neurons of Kv7.4$^{-/-}$ mice might suggest a phenotype of depression. However, this was not the case; no depressive behaviour was observed in Kv7.4$^{-/-}$ mice, and Kv7.4$^{-/-}$ mice developed depression behaviour after being subjected to the stressful stimulation. This indicates that the elevated VTA neuronal excitability is essential but not sufficient for inducing the depression behaviour, and therefore, additional factors, such as corticotrophin release factor (Walsh and Han, 2011), may be necessary. Thus, a stress-context is a precondition for the involvement of VTA DA neurons in the development of depressive behaviour (Chaudhury *et al.*, 2013).

The role of VTA DA neuronal activity in the development of depression raises another question: could the reduced expression/activity of K^+ channels (including that of Kv7 induced, for example, by stress) (Zhou *et al.*, 2016) be a causative factor in the altered firing of VTA DA neurons and the depression-like behaviours related to such altered firing? The results

found thus far suggest that this may be the case. Earlier studies showed that elevated expression/activity of K^+ channels (including Kv7.3/KCNQ3) could be responsible for the lack of susceptibility in a subpopulation of mice that do not develop depression-like behaviour in the social defeat paradigm (Friedman *et al.,* 2014; Krishnan *et al.*, 2007; Friedman *et al.*, 2016). In the current study, we found that the mRNA and protein expression of Kv7.4 were lowered in SUS mice compared with UNSUS mice. Thus, our study suggests that the down-regulation of Kv7.4 abundance is possibly among the causative factors of changes in the excitability of VTA DA neurons, which determines depressive behaviours (Chaudhury *et al.*, 2013; Tye *et al.,* 2013).

It has to be noted that our findings were obtained with the use of a single depression model. Different models of depression may involve different neuronal mechanisms, including the activity of VTA DA neurons (e.g. reduced activity of VTA DA neuron in the mice depression model of the unpredictable chronic mild stress, Chaudhury *et al.*, 2013; Tye *et al*., 2013). This may underlie the complexity of major depression demonstrated in clinical patients and their heterogeneous responses to antidepressants. Therefore, future studies are necessary to test if the mechanisms discovered here contribute to development of depression in other animal models and in human patients. Nevertheless, targeting a causal molecular mechanism of depression (such as a loss of functional activity of Kv7.4), rather than fighting symptoms of the disease might provide a better strategy for development of new antidepressants.

In summary, in this study, we provide strong evidence that Kv7.4 is a key modulator of VTA DA neuronal excitability participating in the development of depressive behaviour. Furthermore, selective targeting of Kv7.4 in VTA DA neurons with drugs such as fasudil presents a potential new strategy for the treatment of major depressive disorder..

Acknowledgment

This work was supported by the National Basic Research Program (2013CB531302) and the National Natural Science Foundation of China (31270882) grants to HZ, and Natural sciences fund of Shandong (ZR2013CQ033). We thank Han Hao for expert technical assistance.

Conflict of Interest

The authors declare no financial and non-financial competing interests.

Reference

Alexander SP, Catterall WA, Kelly E, Marrion N, Peters JA, Benson HE, et al. (2016). The concise guide to pharmacology 2015/16: voltage-gated ion channels. British Journal of Pharmacology, 172: 5904-5941. doi: 10.1111/bph.13349

Barbara J, Han MH (2016). Diversity of Dopaminergic Neural Circuits in Response to Drug Exposure. Neuropsychopharmacology Official Publication of the American College of Neuropsychopharmacology 41**:** 2424-2446. doi: 10.1038/npp.2016.32

Borsotto M, Veyssiere J, Moha Ou Maati H, Devader C, Mazella J, Heurteaux C (2015). Targeting two-pore domain K(+) channels TREK-1 and TASK-3 for the treatment of depression: a new therapeutic concept. Br J Pharmacol 172**:** 771-784. doi:10.1111/bph.12953

Brown DA, Passmore GM (2009). Neural KCNQ (Kv7) channels. Br J Pharmacol 156**:** 1185-1195. doi: 10.1111/j.1476-5381.2009.00111.

Burlet S, Tyler CJ, Leonard CS (2002). Direct and indirect excitation of laterodorsal tegmental neurons by Hypocretin/Orexin peptides: implications for wakefulness and narcolepsy. J Neurosci 22**:** 2862-2872. doi:20026234

Cao JL, Covington HE, 3rd, Friedman AK, Wilkinson MB, Walsh JJ, Cooper DC, et al. (2010). Mesolimbic dopamine neurons in the brain reward circuit mediate susceptibility to social defeat and antidepressant action. J Neurosci 30**:** 16453-16458. doi: 10.1523/JNEUROSCI.3177-10.2010

Chaudhury D, Walsh JJ, Friedman AK, Juarez B, Ku SM, Koo JW, et al. (2013). Rapid regulation of depression-related behaviours by control of midbrain dopamine neurons. Nature 493**:** 532-536. doi: 10.1038/nature11713

Creed M, Kaufling J, Fois GR, Jalabert M, Yuan T, Lüscher C, et al. (2016). Cocaine Exposure Enhances the Activity of Ventral Tegmental Area Dopamine Neurons via Calcium-Impermeable NMDARs. Journal of Neuroscience the Official Journal of the Society for Neuroscience 36**:** 10759-10768. doi: 10.1523/JNEUROSCI.1703-16.2016

Curtis MJ, Bond RA, Spina D, Ahluwalia A, Alexander SPA, Giembycz MA, et al. (2015). Experimental design and analysis and their reporting: new guidance for publication in BJP. British Journal of Pharmacology 172: 3461-3471. doi: 10.1111/bph.12856

Drion G, Bonjean M, Waroux O, Scuvee-Moreau J, Liegeois JF, Sejnowski TJ, et al. (2010). M-type channels selectively control bursting in rat dopaminergic neurons. Eur J Neurosci 31**:** 827-835. doi: 10.1111/j.1460-9568.2010.07107.x

Dunlop BW, Nemeroff CB (2007). The role of dopamine in the pathophysiology of depression. Arch Gen Psychiatry 64**:** 327-337. doi: 10.1001/archpsyc.64.3.327

Franklin KBJ, Paxinos G (2001). The Mouse Brain: In Stereotaxic Coordinates. edn. Academic Press.

Friedman AK, Juarez B, Ku SM, Zhang H, Calizo RC, Walsh JJ, et al. (2016). KCNQ channel openers reverse depressive symptoms via an active resilience mechanism. Nature Communications 24 (7):11671. doi: 10.1038/ncomms11671

Friedman AK, Walsh JJ, Juarez B, Ku SM, Chaudhury D, Wang J, et al. (2014). Enhancing depression mechanisms in midbrain dopamine neurons achieves homeostatic resilience. Science 344**:** 313-319. doi: 10.1126/science.1249240

Gamper N, Shapiro MS. KCNQ Channels. (2015) In: Zheng J, Trudeau MC, Armstrong C, Hille B, Zagotta WN, Jan L, Catterall W, Hoshi T, Nichols CG, Goldstein SAN. Handbook of Ion Channels. CRC Press, Biophysics. pp 275-301

Gershon AA, Vishne T, Grunhaus L (2007). Dopamine D2-like receptors and the antidepressant response. Biol Psychiatry 61**:** 145-153. doi: 10.1016/j.biopsych.2006.05.031

Grace AA, Floresco SB, Goto Y, Lodge DJ (2007). Regulation of firing of dopaminergic neurons and control of goal-directed behaviours. Trends Neurosci 30**:** 220-227. doi: 10.1016/j.tins.2007.03.003

Hansen HH, Waroux O, Seutin V, Jentsch TJ, Aznar S, Mikkelsen JD (2008). Kv7 channels: interaction with dopaminergic and serotonergic neurotransmission in the CNS. J Physiol 586**:** 1823-1832. doi: 10.1113/jphysiol.2007.149450

Hansen HH, Ebbesen C, Mathiesen C, Weikop P, Ronn LC, Waroux O, et al. (2006). The KCNQ channel opener retigabine inhibits the activity of mesencephalic dopaminergic systems of the rat. J Pharmacol Exp Ther 318**:** 1006-1019. doi: 10.1124/jpet.106.106757

Hayashi H, Iwata M, Tsuchimori N, Matsumoto T (2014). Activation of peripheral KCNQ channels attenuates inflammatory pain. Mol Pain 10**:** 15. doi: 10.1186/1744-8069-10-15

Heurteaux C, Lucas G, Guy N, El YM, Thümmler S, Peng XD, et al. (2006). Deletion of the background potassium channel TREK-1 results in a depression-resistant phenotype. Nature Neuroscience 9**:** 1134-1141. doi: 10.1038/nn1749

Jentsch TJ (2000). Neuronal KCNQ potassium channels: physiology and role in disease. Nat Rev Neurosci 1**:** 21-30. doi:10.1038/35036198

Kilkenny C, Browne W, Cuthill IC, Emerson M, Altman DG (2011). Animal research: reporting in vivo experiments|[mdash]|The ARRIVE Guidelines. Journal of Cerebral Blood Flow & Metabolism Official Journal of the International Society of Cerebral Blood Flow & Metabolism 31**:** 991.

Koyama S, Appel SB (2006). Characterization of M-current in ventral tegmental area dopamine neurons. J Neurophysiol 96**:** 535-543. doi: 10.1152/jn.00574.2005

Krishnan V, Han MH, Graham DL, Berton O, Renthal W, Russo SJ, et al. (2007). Molecular adaptations underlying susceptibility and resistance to social defeat in brain reward regions. Cell 131**:** 391-404. doi: 10.1016/j.cell.2007.09.018

Kumar M, Reed N, Liu R, Aizenman E, Wipf P, Tzounopoulos T (2016). Synthesis and Evaluation of Potent KCNQ2/3-specific Channel Activators. Molecular Pharmacology. doi: 10.1124/mol.115.103200

Mameli-Engvall M, Evrard A, Pons S, Maskos U, Svensson TH, Changeux JP, et al. (2006). Hierarchical Control of Dopamine Neuron-Firing Patterns by Nicotinic Receptors. Neuron 50**:** 911-921. doi: 10.1523/JNEUROSCI.1958-08.2008

Mazella J, Petrault O, Lucas G, Deval E, Beraud-Dufour S, Gandin C, et al. (2010). Spadin, a sortilin-derived peptide, targeting rodent TREK-1 channels: a new concept in the antidepressant drug design. PLoS Biol 8**:** e1000355. doi:10.1371/journal.pbio.1000355

Mcgrath JC, Lilley E (2015). Implementing guidelines on reporting research using animals (ARRIVE etc.): new requirements for publication in BJP. British Journal of Pharmacology 172: 3189. doi: 10.1111/bph.12955

Munoz MB, Slesinger PA (2004). Sorting nexin 27 regulation of G protein-gated inwardly rectifying K(+) channels attenuates in vivo cocaine response. Neuron 82**:** 659-669. doi: 10.1016/j.neuron.2014.03.011

Nair-Roberts RG, Chatelain-Badie SD, Benson E, White-Cooper H, Bolam JP, Ungless MA (2008). Stereological estimates of dopaminergic, GABAergic and glutamatergic neurons in the ventral tegmental area, substantia nigra and retrorubral field in the rat. Neuroscience 152**:**

1024-1031. doi: 10.1016/j.neuroscience.2008.01.046

Neuhoff H, Neu A, Liss B, Roeper J (2002). I(h) channels contribute to the different functional properties of identified dopaminergic subpopulations in the midbrain. J Neurosci 22**:** 1290-1302. doi:22/4/1290 [pii]

Overstreet DH, Wegener G (2013). The flinders sensitive line rat model of depression--25 years and still producing. Pharmacol Rev 65**:** 143-155. doi: 10.1124/pr.111.005397

Padgett C, Lalive A, Tan K, Terunuma M, Munoz M, Pangalos M, et al. (2012). Methamphetamine-Evoked Depression of GABA B Receptor Signaling in GABA Neurons of the VTA. Neuron 73**:** 978-989. doi: 10.1016/j.neuron.2011.12.031

Schultz W (2007). Multiple dopamine functions at different time courses. Annu Rev Neurosci 30**:** 259-288. doi: 10.1146/annurev.neuro.28.061604.135722

Shabat-Simon M, Levy D, Amir A, Rehavi M, Zangen A (2008). Dissociation between rewarding and psychomotor effects of opiates: differential roles for glutamate receptors within anterior and posterior portions of the ventral tegmental area. Journal of Neuroscience the Official Journal of the Society for Neuroscience 28**:** 8406-8416. doi: 10.1523/JNEUROSCI.1958-08.2008

Southan C, Sharman JL, Benson HE, Faccenda E, Pawson AJ, Alexander SP et al. (2016). The IUPHAR/BPS Guide to PHARMACOLOGY in 2016: towards curated quantitative interactions between 1300 protein targets and 6000 ligands. Nucl Acids Res 44: doi: 1054-1068.

Tatjana Kharkovets KD, Hannes Maier, Michaela Schweizer, Darina Khimich, Régis Nouvian, Vitya Vardanyan, Rudolf Leuwer, Tobias Moser, Thomas J Jentsch (2006). Mice with altered KCNQ4 K+ channels implicate sensory outer hair cells in human progressive

deafness. Embo Journal 25**:** 642-652. doi: 10.1038/sj.emboj.7600951

Tatulian L, Delmas P, Abogadie FC, Brown DA (2001). Activation of expressed KCNQ potassium currents and native neuronal M-type potassium currents by the anti-convulsant drug retigabine. J Neurosci 21**:** 5535-5545. doi:21/15/5535 [pii]

Tsai HC, Zhang F, Adamantidis A, Stuber GD, Bonci A, de Lecea L, et al. (2009). Phasic firing in dopaminergic neurons is sufficient for behavioural conditioning. Science 324**:** 1080-1084. doi: 10.1126/science.1168878

Tye KM, Mirzabekov JJ, Warden MR, Ferenczi EA, Tsai HC, Finkelstein J, et al. (2013). Dopamine neurons modulate neural encoding and expression of depression-related behaviour. Nature 493**:** 537-541. doi: 10.1038/nature11740

Uehata M, Ishizaki T, Satoh H, Ono T, Kawahara T, Morishita T, et al. (1997). Calcium sensitization of smooth muscle mediated by a Rho-associated protein kinase in hypertension. Nature 389**:** 990-994. doi:10.1038/40187

Ungless MA, Magill PJ, Bolam JP (2004). Uniform inhibition of dopamine neurons in the ventral tegmental area by aversive stimuli. Science 303**:** 2040-2042. doi: 10.1126/science.1093360

Veyssiere J, Moha Ou Maati H, Mazella J, Gaudriault G, Moreno S, Heurteaux C, et al. (2015). Retroinverso analogs of spadin display increased antidepressant effects. Psychopharmacology (Berl) 232**:** 561-574. doi:10.1007/s00213-014-3683-2

Walsh JJ, Han MH (2011). The heterogeneity of ventral tegmental area neurons: Projection functions in a mood-related context. Neuroscience 282C**:** 101-108. doi: 10.1016/j.neuroscience.2014.06.006

Wang HS, Pan Z, Shi W, Brown BS, Wymore RS, Cohen IS, et al. (1998). KCNQ2 and KCNQ3 potassium channel subunits: molecular correlates of the M-channel. Science 282**:** 1890-1893. doi: 10.1126/science.282.5395.1890

Williams SR, Wozny C (2011). Errors in the measurement of voltage-activated ion channels in cell-attached patch-clamp recordings. Nat Commun 2**:** 242. doi: 10.1038/ncomms1225

Wong ML, Licinio J (2001). Research and treatment approaches to depression. Nat Rev Neurosci 2**:** 343-351. doi: 10.1038/35072566

Zhang X, An H, Li J, Zhang Y, Liu Y, Jia Z, et al. (2016). Selective activation of vascular Kv7.4/Kv7.5 K+ channels by fasudil contributes to its vasorelaxant effect. British Journal of Pharmacology. doi: 10.1111/bph.13639

Zhou JJ, Gao Y, Kosten TA, Zhao Z, Li DP (2016). Acute stress diminishes M-current contributing to elevated activity of hypothalamic-pituitary-adrenal axis. Neuropharmacology. 114:67-76. doi: 10.1016/j.neuropharm.2016.11.024

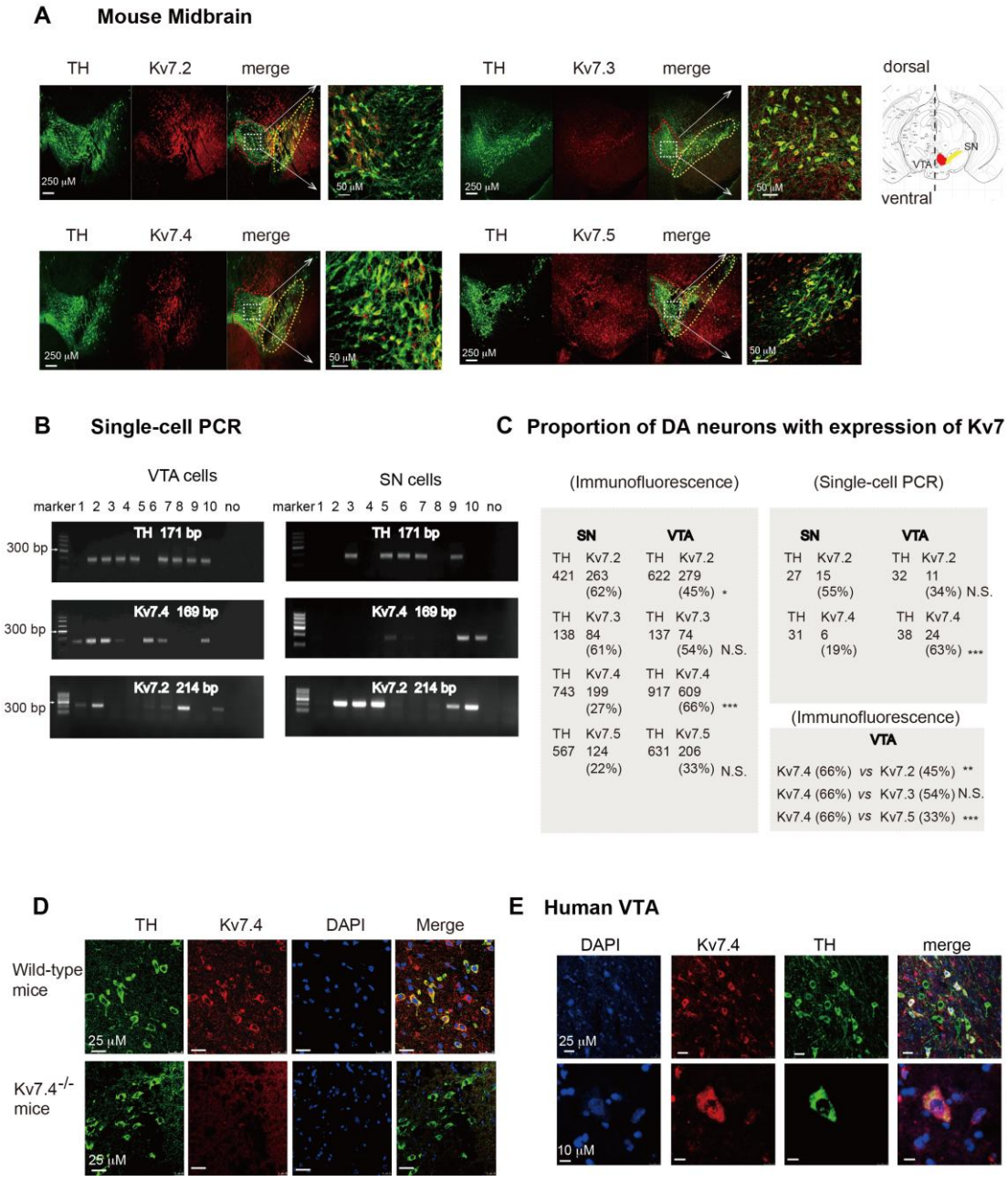

Fig. 1

The expression of Kv7 channels in the midbrain. (A) Representative immunofluorescence images of the co-expression of Kv7 subunits (Kv7.2, Kv7.3, Kv7.4 and Kv7.5) and tyrosine hydroxylase (TH) in themesencephalon of the mice. The ventral tegmental area (VTA) and substantia nigra (SN) are highlighted by the red and yellow dotted circles, respectively, and a zoomed-in area of the VTA is shown by the dotted square and the white arrows. A schematic of the VTA (red) and SN (yellow) areas in the map of a midbrain coronal section is also

shown in the inset on the right. (B) Reverse-transcription (RT) PCR analysis of single neurons from VTA and SN brain slices. The lane numbers correspond to individual neurons; “no” denotes the negative control in which no template (neuronal lysate) was added in the RT-PCR reaction. The expected sizes of the DNA products for tyrosine hydroxylase (TH) and Kv7s are shown. (C) Proportions of dopamine (DA) neurons (TH-positive) expressing individual Kv7 subunits, analysed for protein (immunofluorescence) and mRNA (single cell PCR) levels. (D) Immunofluroscence identification of Kv7.4 (red) and TH (green) expression in the VTA of wild-type and Kv7.4 knockout ($Kv7.4^{-/-}$) mice. (E) Kv7.4 (red) and TH (green) in a VTA slice from a human brain

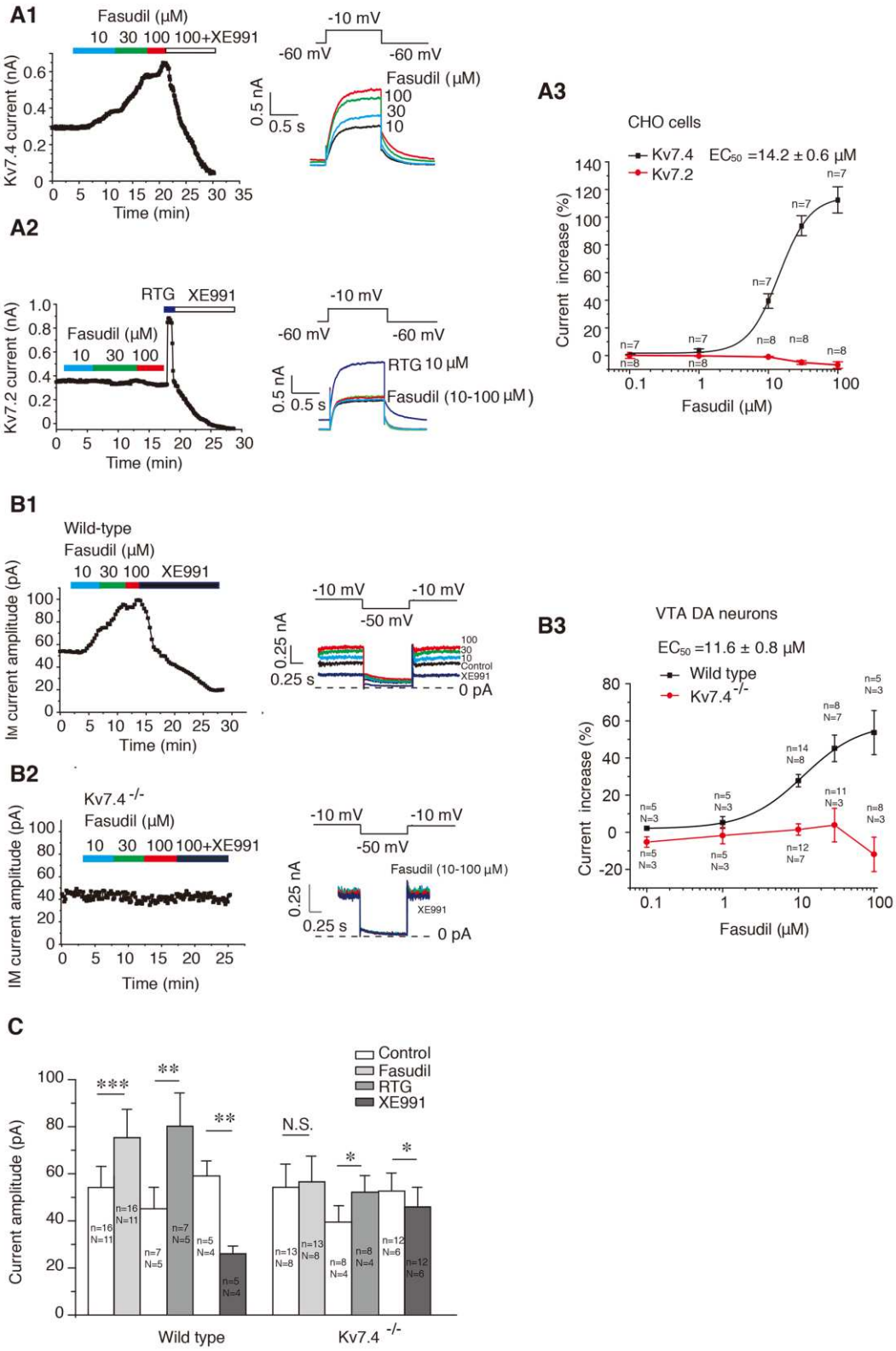

Fig. 2

Fasudil selectively activates Kv7.4 currents in CHO cells and VTA DA neurons. Whole-cell patch clamp recordings from CHO cells and DA neurons in brain slices. (A1) Fasudil

enhanced the currents of Kv7.4 channels stably expressed in CHO cells. The time course shows on the left is the time lapsed deactivating tail current amplitudes recorded at -60 mV from a depolarizing steps to -10 mV in 20 s intervals. Example current traces in the absence or presence of 10 μM, 30 μM or 100 μM fasudil are shown on the right with the voltage pulse protocol shown in the inset above the traces. (A2) Fasudil (10 μM, 30 μM or 100 μM) did not affect Kv7.2 currents, while RTG (10 μM) induced a 3-fold augmentation. (A3) Concentration-response curve for the effect of fasudil on Kv7.4 currents fitted with a logistic function; EC_{50} = 14.2 ± 0.6 μM. Fasudil had no detectable effect on the Kv7.2 currents. (B) Kv7/M currents recorded from VTA DA neurons from wild-type and $Kv7.4^{-/-}$ mice. (B1) shows the effects of fasudil (10 μM, 30 μM or 100 μM) on the XE991-sensitive (3 μM) deactivating tail currents measured at -50 mV (left). The protocol used to induce Kv7/M currents and the corresponding current traces are shown in the right panel. (B3) The concentration-response relationships of the effect of fasudil on Kv7/M currents in DA neurons fitted with the logistic function; EC_{50} = 11.6 ± 0.8 μM. (C) The summarized effects of fasudil, RTG and XE991 on Kv7/M current amplitude in VTA DA neurons from wild type and $Kv7.4^{-/-}$ mice * $P < 0.05$, paired sample Wilcoxon signed ranks test for fasudil, paired t-test for XE991 and RTG; n is the number of cells and N is the number of animals.

.

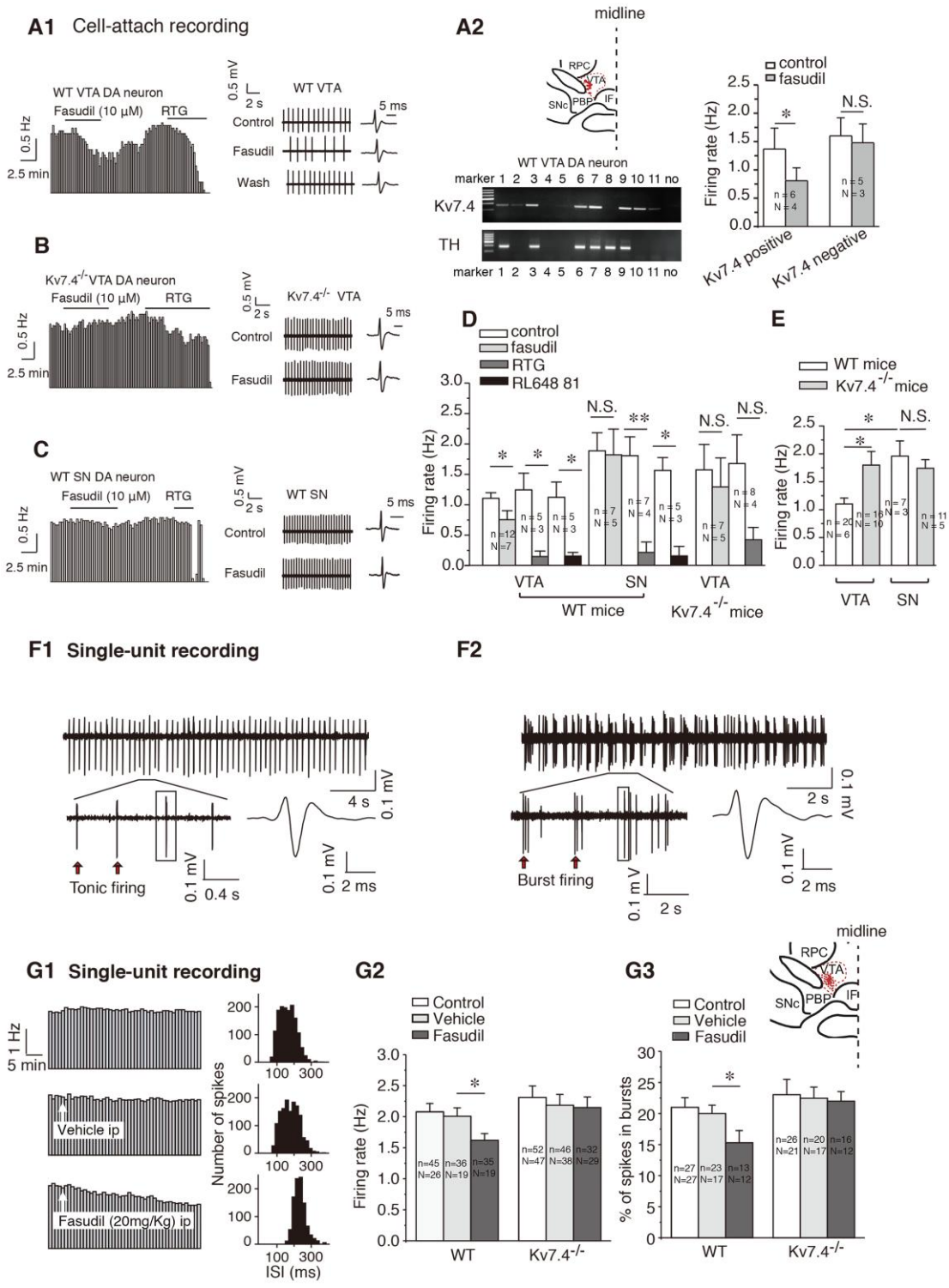

Fig. 3

Fasudil decreases spontaneous firing of VTA DA neurons. (A-C) Cell-attached recording of spontaneous firing of DA neurons from VTA and SN areas. (A1) Effect of fasudil (10 μM) and RTG (10 μM) on the spontaneous firing frequency of VTA DA neurons from wild type

mice. Example recordings and action potential waveforms are shown on the right. (A2) Left: Post-recording single-cell PCR shows the presence of Kv7.4 in TH-positive neurons. The inset on the top shows a map of a coronal midbrain slice indicating the location of neurons that were recorded and subsequently analysed with RT-PCR indicated (red dots). Right panel summarizes the effects of fasudil on the firing frequency of Kv7.4-positive and Kv7.4-negative TH-expressing neurons. (B) Effect of fasudil and RTG on spontaneous firing of VTA DA neurons from a $Kv7.4^{-/-}$ mouse. (C) Effect of fasudil and RTG on the spontaneous firing of SN DA neurons from a wild-type mouse. (D) Summary of the effects of fasudil, RTG and a Kv7.2 selective activator RL-648 81 on spontaneous firing frequency of VTA and SN DA neurons. * $P < 0.05$, N.S., not significant, paired t-test. (E) Summary of the spontaneous firing frequencies of VTA and SN DA neurons from wild type and $Kv7.4^{-/-}$ mice. (F) *In vivo* single unit recording of spontaneously firing of VTA DA neurons. Tonic (F1) and burst (F2) firing DA neurons are exemplified. (G1) The time course of the firing frequency and the ISI of DA neurons following intraperitoneal injection (i.p.) of fasudil (20 $mg \cdot kg^{-1}$) or vehicle (0.9% saline). The average firing frequency within 1 min bins is plotted against time. (G2) Summary of the effects of fasudil on the firing frequency recorded in experiments similar to those shown in G1. * $P < 0.05$, one-way ANOVA. (G3) Summary of the effects of fasudil on the incidence of burst firing (percentage of spikes in bursts). * $P < 0.05$, one-way ANOVA. n is the number of cells and N is the number of animals.

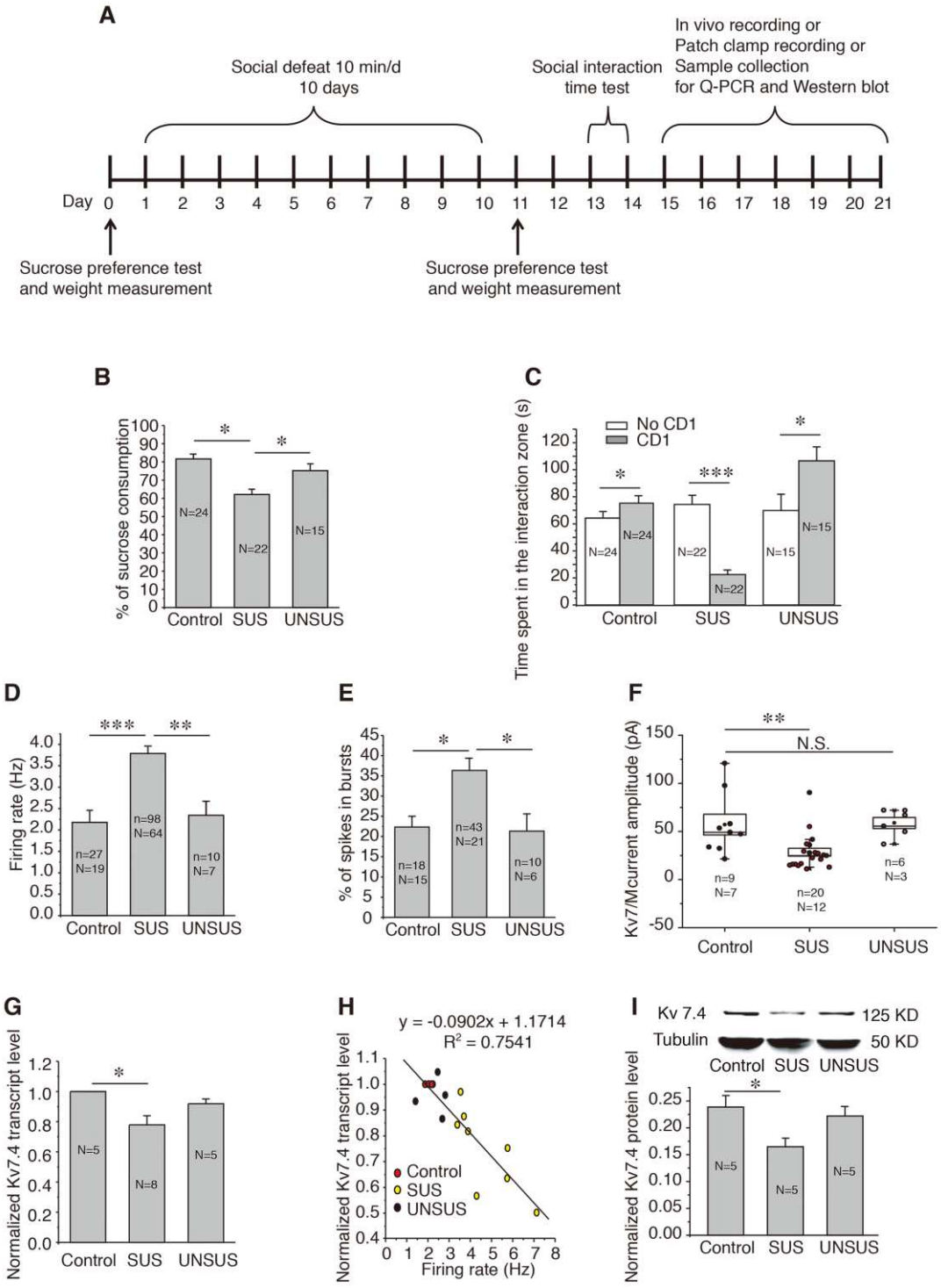

Fig. 4

The role of Kv7.4 on the increased activity of VTA DA neurons in the social defeat model of depression. (A) Timeline of the chronic social defeat model. (B) The sucrose preference test. SUS-susceptible mice, UNSUS-unsusceptible mice (for detail see Methods). * $P < 0.05$, one-way ANOVA. (C) Social interaction test. The time that the test mice spent in the

interaction zone in the absence ('No CD1') or presence ('CD1') of an unfamiliar CD1 mouse. * $P < 0.05$, paired t-test. (D) Summary of VTA DA neuronal firing frequenciesof the *in vivo* single-unit recordings from control, SUS and UNSUS mice. (E) Percentage of spikes in bursts during the spontaneous firing of VTA DA neurons from control, SUS and UNSUS mice. * $P < 0.05$, one-way ANOVA. (F) Kv7.4/M current amplitudes of VTA DA neurons from control, SUS and UNSUS mice, recorded using whole-cell patch clamp recording. N.S., not significant, Kruskal-Wallis ANOVA and Mann-Whitney test. (G) Kv7.4 mRNA expression measured with Q-PCR. * $P < 0.05$, one-way ANOVA. (H) Correlation analysis of Kv7.4 mRNA levels and the firing frequency of the VTA DA neurons ($P = 0.0000129$, y = -0.0902x + 1.1714, R2 = 0.7541; linear correlation analysis). The firing of VTA DA neurons was recorded using single unit recording. Each point in the chart represented a result from a separate mouse. (I) Kv7.4 protein levels measured using western blot. * $P < 0.05$, one-way ANOVA; n is the number of cells and N is the number of animals.

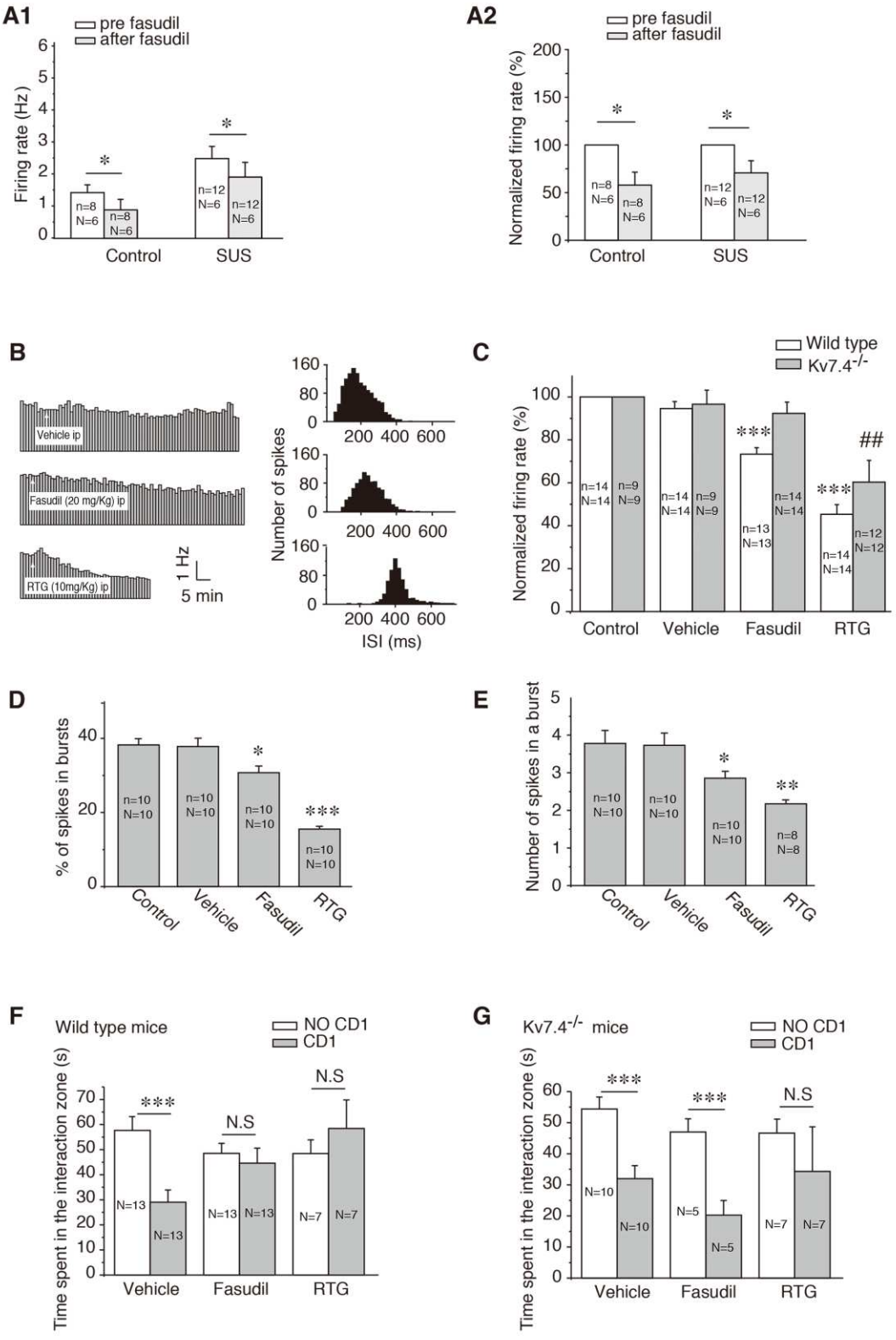

Fig. 5.

Fasudil reverses the depression-like behaviour in the mice developing social defeat through the activation of Kv7.4. (A1) Effect of fasudil on the spontaneous firing rate of VTA DA

neurons from control and SUS mice from cell-attached recording of DA neurons in VTA slices. * $P < 0.05$, paired t-test. (A2) Normalized firing frequency based on the data shown in A1. * $P < 0.05$, N.S., not significant, one sample Wilcoxon signed ranks test. (B) Effect of fasudil (20 $mg \cdot kg^{-1}$, i.p.), RTG (10 $mg \cdot kg^{-1}$, i.p.) or vehicle (0.9% saline) on the firing frequency and the ISI of VTA DA neurons recorded using *in vivo* single unit recording. The average firing frequency within 1 min bins is plotted against time. (C) Summary of the effect of fasudil and RTG on the firing frequency of VTA DA neurons from WT and Kv7.4$^{-/-}$ mice. (D) Effect of fasudil and RTG on the incidence of burst firing. * $P < 0.05$, one-way ANOVA. (E) Effect of fasudil and RTG on the number of spikes in a burst. * $P < 0.05$; one-way ANOVA. (F) Effect of vehicle, fasudil and RTG on the social interaction time of social defeat WT mice. N.S., not significant, paired t-test. (G) Effect of vehicle, fasudil and RTG on the social interaction time of social defeat Kv7.4$^{-/-}$ mice. N.S., not significant, paired t-test. n is the number of cells and N is the number of animals.

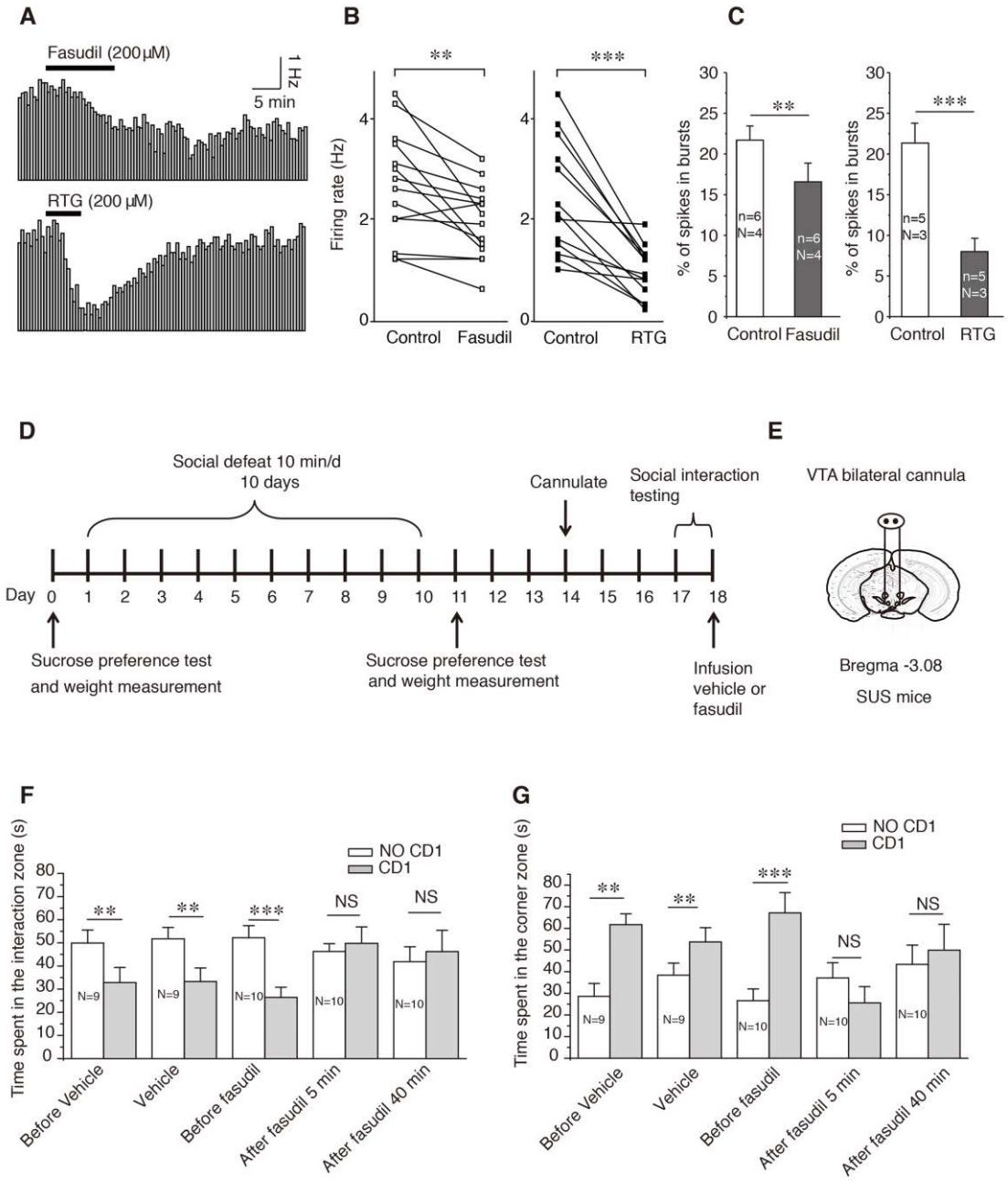

Fig. 6.

Microinfusion of fasudil into the VTA decreases the spontaneous firing of VTA DA neurons and reverses depression-like behaviour. (A) The time courses of the firing frequency of DA neurons following local injection of fasudil (200 μM; top) or RTG (200 μM; bottom) into the VTA of mice. (B) Summary of the effects of fasudil and RTG on the firing frequency recorded in experiments similar to those shown in A. (C) Summary of the effects of fasudil and RTG on the incidence of burst firing (percentage of spikes in bursts). (D) Timeline for

the establishment of the social defeat model, the interaction test and the microinfusion of drugs. (E) Schematic depiction of cannula placement for direct microinjections of drugs into the VTA. (F and G) Summary of the effect of fasudil on social interaction: the time spent in the interaction zone (F) and in the corner zone (G) Tests were performed 5 and 40 min after the direct VTA infusion of fasudil (0.08 μg, 200 μM, 0.4 μl). N.S, not significant, paired t-test. N is the number of animals tested.

List of Hyperlinks for crosschecking

key protein and ligend

K^+ channels

Kv7.4

Kv7.2

Kv7.3

fasudil

retigabine

XE991